

FERMILAB-Pub-92/318-A

Imperial/TP/92-93/03
26th October, 1992

Following a “collapsing” wavefunction

Andreas Albrecht

NASA/Fermilab Astrophysics Center
P.O.B. 500, Batavia, IL 60510

and

Blackett Laboratory*, Imperial College, Prince Consort Road
London SW7 2BZ U.K.

Abstract

I study the quantum mechanics of a spin interacting with an “apparatus”. Although the evolution of the whole system is unitary, the spin evolution is not. The system is chosen so that the spin exhibits loss of quantum coherence, or “wavefunction collapse”, of the sort usually associated with a quantum measurement. The system is analyzed from the point of view of the spin density matrix (or “Schmidt paths”), and also using the consistent histories approach. These two points of view are contrasted with each other. Connections between the results and the form of the Hamiltonian are discussed in detail.

1 Introduction

A cosmologist must face the the issue of interpreting quantum mechanics without the benefit of an outside classical observer. By definition, there is

*Permanent address since August 1992

Submitted to Physical Review D



nothing “outside” the universe! The traditional role of an outside classical observer is to cause “wavefunction collapse”. This process causes a definite outcome of a quantum measurement to be realized, with the probability for a given outcome determined by the initial wavefunction of the system being measured. It is common to view this process as something that can not be described by a wavefunction evolving according to a Schrödinger equation, but which instead must be implemented “by hand”.

There is a growing understanding [1, 2, 3, 4, 5, 6, 7, 8, 9, 10] that the essential features of wavefunction collapse *can* be present in systems whose evolution is entirely unitary. The key is the inclusion of an “environment” or “apparatus” within the Hilbert space being studied. A *subsystem* can then exhibit the non-unitary aspects of wavefunction collapse even though the system as a whole evolves unitarily. The wavefunction can then divide up into a number of different terms, each of which reflect a different “outcome”. When there is negligible interference among the different terms during subsequent evolution, the “definiteness” of the outcome is realized in a restricted sense: Each term evolves as if the others were “not there”, so a subsystem state within a given term evolves with “certainty” that its corresponding outcome is the only one. None the less, the total wavefunction describes all possible outcomes, and one is never singled out.

Some people object to all the “extra baggage” or “many worlds”[11] which result from retaining all possible outcomes. However, this approach has the advantage of allowing quantum mechanics to operate in a much more fundamental way, and *predict* which subsystems can play the role of classical observers. Unless the predictions are falsified, this approach can never be shown to be wrong.

In what follows I present a simple toy system which is designed to illustrate the essential features of a quantum measurement. A very primitive “apparatus” is coupled to a two state “spin”. The whole spin-apparatus system evolves unitarily and remains in a pure state, even as the two subsystems exhibit the non-unitary evolution associated with the measurement. Both the “consistent histories” point of view, and a more conventional point of view (using reduced density matrices or “Schmidt paths”) are used to analyze the same process. The connections between the two points of view are discussed.

This paper is an expanded version of a talk presented at the “Workshop on time asymmetry” in Mazagon Spain [12]. The results are the same, but in

this paper I describe the Hamiltonian, and explore in detail the relationship between the results and my choice of Hamiltonian. The purpose is develop some intuition as to what attributes make a “good classical observer”.

The organization of this paper is as follow: Section 2 presents some mathematical tools. Section 3 introduces the toy model and illustrates what it has to do with a quantum measurement by analogy with the double slit experiment. Section 4 shows the behavior of the toy model in more quantitative detail. Section 5 introduces the “consistent histories” point of view, and section 6 applies this point of view to the toy model. Section 7 explains specifically how the form of the Hamiltonian allows the density matrix evolution described in section 4 to be achieved. Section 8 explains how the form of the Hamiltonian allows the consistent histories described in Section 6 to be achieved. Section 9 discusses the relationship between the Schmidt paths and consistent histories. Section 10 explores the fundamental role played by the statistical “arrow of time” in the processes under study. Conclusions are presented in Section 11, and a number of technical results are presented in the Appendices. Units in which $\hbar = 1$ are used throughout.

2 Tools

The focus of this paper is the evolution of the spin and apparatus subsystems from pure into mixed states due to correlations being set up between the subsystems. The “Schmidt decomposition” provides a useful tool for dealing with these issues, and it will be used throughout this paper.

If a closed system in a pure state $|\psi\rangle$ is divided into two subsystems, one might want to think about $|\psi\rangle$'s of the form

$$|\psi\rangle = |\psi\rangle_1 \otimes |\psi\rangle_2. \quad (1)$$

One could then say subsystem 1 is in the pure state $|\psi\rangle_1$, and subsystem 2 is in the pure state $|\psi\rangle_2$. However, this “direct product” form for $|\psi\rangle$ is far from general. A general $|\psi\rangle$ would look like:

$$|\psi\rangle = \sum_{i,j} \alpha_{ij} |i\rangle_1 \otimes |j\rangle_2 \quad (2)$$

where $\{|i\rangle_1\}$ and $\{|j\rangle_2\}$ span the two respective subspaces. Then one can not talk about pure states for subsystems 1 and 2. However, one can say

something along these lines if $|\psi\rangle$ takes the special form:

$$|\psi\rangle = \sum_i \alpha_i |i\rangle_1 \otimes |i\rangle_2 \quad (3)$$

for some orthonormal sets $\{|i\rangle_1\}$ and $\{|i\rangle_2\}$. This form is special because there is only one summation, and each state for system 1 is uniquely correlated with a specific state for system 2. The reduced density matrix of system 2 is then

$$\rho_2 \equiv \text{tr}_1 (|\psi\rangle\langle\psi|) = \sum_i \alpha_i^* \alpha_i |i\rangle_2 \langle i| \quad (4)$$

which is *diagonal* in the $\{|i\rangle_2\}$ basis. The result is that the probability assigned to any state $|x\rangle_2$ of the spin is

$$\langle x|\rho_2|x\rangle = \sum_i \alpha_i^* \alpha_i |\langle x|i\rangle_2|^2, \quad (5)$$

which is an incoherent sum over the probabilities of each state $|i\rangle_2$, weighted by the probability $\alpha_i^* \alpha_i$ assigned to that particular state.

One can thus regard system 2 to be in state $|i\rangle_2$ with probability $\alpha_i^* \alpha_i$. Although quantum mechanics allows one to assign probabilities for the spin to be in any state, the basis in which ρ_2 is diagonal is special, because only in that basis does any matrix element of ρ_2 take the form of an *incoherent* sum as depicted in Eq (5) (with no interference terms like $\langle x|i\rangle_2 \langle j|x\rangle$).

It turns out that the “special form” of Eq (3) can always be realized. It is called “Schmidt” form, and follows directly from the fact that any density matrix can be diagonalized. The Schmidt bases, $\{|i\rangle_1^S\}$ and $\{|i\rangle_2^S\}$, are the eigenstates of the reduced density matrices ρ_1 and ρ_2 , and $\alpha_i = \sqrt{p_i}$, where p_i are the eigenvalues (ρ_1 and ρ_2 have the same eigenvalues, and the larger one has additional zero eigenvalues). For more discussion of the Schmidt decomposition see [13, 14, 1, 15, 16, 17, 18]. Ref [13] contains the original mathematical result, and a brief proof is offered in [18].

The Schmidt decomposition allows one to expose precisely which correlations are present between two subsystems. The special form of Eq 3 shows that state $|1\rangle_1$ is uniquely correlated with state $|1\rangle_2$ and so on. It also allows one to make the clearest possible statement of the “state of a subsystem”, by providing the eigenstates and eigenvalues of the relevant reduced density matrix.

3 The toy model

3.1 Defining the model

The toy model discussed here is two state “spin”(system 2) coupled to a modest sized “apparatus” (system 1). The Hamiltonian is the same one used in [18], which takes the form

$$H = H_1 \otimes I_2 + I_1 \otimes H_2 + H_I \quad (6)$$

Where I_k represents the unit operator in the space of subsystem k . The first two terms give self Hamiltonians of the apparatus and spin respectively, and the last term gives the interaction between spin and apparatus.

For this article I have chosen the parameters so that the interaction Hamiltonian dominates over the self-Hamiltonians of the two subsystems. (Specifically $E_1 = E_2 = 0.1$ and $E_I = 10$ in the notation of [18].) The size of the system 1 is $n_1 = 25$ here, as opposed to $n_1 = 12$ in [18].

The interaction Hamiltonian is:

$$H_I = E_I (|\uparrow\rangle \langle \uparrow| \otimes H_1^\uparrow + |\downarrow\rangle \langle \downarrow| \otimes H_1^\downarrow) \quad (7)$$

where H_1^\uparrow and H_1^\downarrow are two *different* random Hermitian matrices in the system 1 subspace. (Each independent real and imaginary part of each element of H_1^\uparrow and H_1^\downarrow is chosen randomly on the interval $[-0.5, 0.5]$.) The random matrices are chosen once and for all at the start of the calculation, so H_I is time independent. For our purposes, the role of the self-Hamiltonians for the subsystems can be described by the statement “the deviation of the total Hamiltonian from H_I is very small”. For more details see [18].

The idea behind the form of H_I is very simple: If the spin is up the apparatus is pushed in one direction by H_1^\uparrow and if the spin is down, the apparatus is pushed in a very different direction by H_1^\downarrow . The goal is to correlate different states in the apparatus with the $|\uparrow\rangle$ and $|\downarrow\rangle$ states for the spin.

3.2 The purpose of the model

The toy model is designed to perform a very specific function: The model should take an initial state of the form

$$|\psi_i\rangle = (a|\uparrow\rangle_2 + b|\downarrow\rangle_2) \otimes |X\rangle_1 \quad (8)$$

and evolve it into the state:

$$|\psi_f\rangle = a|\uparrow\rangle_2 \otimes |Y\rangle_1 + b|\downarrow\rangle_2 \otimes |Z\rangle_1 \quad (9)$$

Where $\langle Y|Z\rangle = 0$. Actual numerical results showing this evolution are presented in Section 4, and a detailed analysis of why this model is able to achieve these results appears in Sections 7.

Both Eqs (8) and (9) are in Schmidt form. Thus one can see that initially the spin (and the apparatus) is in a “pure” state. Later, ρ_2 develops *two* non-zero eigenvalues, so the spin is in a mixed state. The eigenstates of the final spin density matrix are $|\uparrow\rangle$ and $|\downarrow\rangle$. Thus, at the end the spin is clearly no longer in the $a|\uparrow\rangle_2 + b|\downarrow\rangle_2$ state, but it may be said to be in an incoherent superposition of $|\uparrow\rangle$ and $|\downarrow\rangle$. An important feature is that the probabilities assigned to $|\uparrow\rangle$ and $|\downarrow\rangle$ at the end (a^*a and b^*b respectively) are the same as those assigned initially. The only difference is that the initial state is a *coherent* superposition of $|\uparrow\rangle$ and $|\downarrow\rangle$. The choice of $|\uparrow\rangle$ and $|\downarrow\rangle$ as the final eigenstates of the density matrix was built into the dynamics (and the choice of initial state). Although the evolution of the spin is non-unitary (since the eigenvalues of its density matrix change), the evolution of the total spin plus apparatus system is chosen to be completely unitary.

3.3 Analogy with the double slit

What does this have to do with wavefunction collapse? One might expect a parallel description of the standard double slit experiment: After passing through a double slit, an electron wave packet becomes spread out into a distinctive double slit diffraction pattern. At this point the electron is still in a pure state, and it is at this point that I wish to make the analogy with Eq 8, the initial state for the toy system. After interacting with a screen, the electron is certainly not in a pure state, but the electron may be expressed as an incoherent superposition of localized packets. The probability assigned to each packet is the same probability assigned to that location by the original pure electron state. (Extremely low probabilities are assigned at nodes of the double slit pattern, for example.) The loss of coherence of the initial state is due to the setting up of correlations between the electron and the screen. The screen plays the role of system 1 in equation (9) (of course there would be more than two terms in the Schmidt expansion of the electron-screen system).

For each localized packet the screen is in a different orthogonal state. The extent to which the electron density matrix eigenstates tend to be localized packets rather than some other types of states is determined by the nature of the interaction, and the initial state of the screen. It is natural to expect the eigenstates to be localized, due to the local nature of interactions. Because of the correlation between the screen and the electron, one can determine the state of the electron by measuring the state of the screen. In fact, one normally does look at the screen, not at the electron.

There are three key features of the double slit experiment which are present in the toy system. First, the density matrix eigenstates (or Schmidt states) take a particular form after the measurement which is determined by the interactions. This “pointer basis” ([3]) is $\{|\uparrow\rangle, |\downarrow\rangle\}$ in the toy model, and fairly localized wave packet states for the electron in the double slit example.

Second, the probability assigned to each density matrix eigenstate after the measurement corresponds to the same probability assigned to that state in the pre-interaction pure state. For the spin, this results because the coefficients “ a ” and “ b ” are the same in Eqns 8 and 9. For the double slit case, the diffraction pattern is represented in the distribution of density matrix eigenvalues after the interaction. (This is why, after many electrons strike the screen, the diffraction pattern is produced.)

Third, it is very unlikely that the process will reverse itself. For the double slit, it is extremely unlikely that the screen will emit an electron in a double slit diffraction pattern. The reason why the toy model is unlikely to evolve from Eq 9 back to Eq 8 will be discussed in Section 7.

One way the analogy does not work is in the details of the apparatus. The apparatus in the toy model is much less sophisticated than a realistic screen. Although the different “outcomes” of the measurement do get correlated with orthogonal states of the apparatus, the apparatus states do not represent a nice “pointer” or “mark on a screen” which clearly reflects the state of the quantity being measured.

4 Results

Figure 1 shows information about the spin as the whole system evolves. Initially, the state is given by Eq (8), with $a = 0.7, b = 0.3$. In the lower plot, the solid curve gives p_1 , the largest eigenvalue of ρ_2 . It starts out at unity,

as required by the “pure state” form of the initial conditions, and evolves to 0.7, where it holds steady. The dashed curve gives the entropy, S , of the spin ($S \equiv -\text{tr}[\rho_2 \log_2(\rho_2)]$), in units where the maximum possible entropy in unity. The entropy starts out zero and increases. This is always the case when a system evolves from a pure to a mixed state. (Note the the combined “spin \otimes apparatus” system remains in a pure state, so *its* entropy is zero)

In the upper plot, the dashed curve gives the overall probability for the spin to be up, given by $\langle \uparrow | \rho_2 | \uparrow \rangle$. This quantity is a “constant of the motion”. The solid curve gives $|\langle \uparrow | 1 \rangle^S|^2$, where $|1\rangle^S$ is the eigenstate of ρ_2 (or “Schmidt state”) corresponding to the largest eigenvalue.

Since $|1\rangle^S$ belong to a two state Hilbert space, it is completely specified by $|\langle \uparrow | 1 \rangle^S|^2$, up to an overall phase. One can see that as the eigenvalue (p_1) approaches 0.7, the eigenvector becomes essentially $|\uparrow\rangle$. Thus the behavior promised in the previous section (Eqs (8) and (9)) is realized to a good accuracy.

Figure 2 is another representation of the way the eigenstates of ρ_2 evolve. The first row represents $|1\rangle^S$, and the second row represents the other eigenvector. The three columns correspond to three times. The histogram in each plot provides two numbers, $p(\uparrow) \equiv |\langle \uparrow | 1 \rangle|^2$ and $p(\downarrow) \equiv |\langle \downarrow | 1 \rangle|^2$ for the first row, and similarly for the second eigenvector in the second row. In this way one can visualize a “collapsing wavefunction” by following the eigenstates of ρ_2 as they “collapse” onto the $\{|\uparrow\rangle, |\downarrow\rangle\}$ basis.

5 Consistent Histories

I will now make contact with the “consistent histories” or “decoherence functional” approach to quantum mechanics of closed systems. Until now I have been using the wavefunction to assign instantaneous probabilities to different states over a range of times. By contrast, the consistent histories endeavors to assign probabilities to *histories*. Consider two projection operators:

$$\hat{P}_\uparrow \equiv |\uparrow\rangle\langle\uparrow| \otimes I_1; \quad \hat{P}_\downarrow \equiv |\downarrow\rangle\langle\downarrow| \otimes I_1 \quad (10)$$

where I_1 is the identity operator in the apparatus subspace, and $\{|\uparrow\rangle, |\downarrow\rangle\}$ form an orthonormal “projection basis” which spans the spin subspace. These projection operators sum to unity:

$$\hat{P}_\uparrow + \hat{P}_\downarrow = I. \quad (11)$$

One can take the formal expression for the time evolution:

$$|\psi(t)\rangle = e^{-iHt}|\psi(0)\rangle \quad (12)$$

and insert the unit operator $(\hat{P}_\uparrow + \hat{P}_\downarrow)$ at will, resulting, for example, in the identity:

$$|\psi(t)\rangle = (\hat{P}_\uparrow + \hat{P}_\downarrow)e^{-iH(t-t_1)}(\hat{P}_\uparrow + \hat{P}_\downarrow)e^{-iHt_1}|\psi(0)\rangle \quad (13)$$

$$= \hat{P}_\uparrow e^{-iH(t-t_1)}\hat{P}_\uparrow e^{-iHt_1}|\psi(0)\rangle + \hat{P}_\uparrow e^{-iH(t-t_1)}\hat{P}_\downarrow e^{-iHt_1}|\psi(0)\rangle \\ + \hat{P}_\downarrow e^{-iH(t-t_1)}\hat{P}_\uparrow e^{-iHt_1}|\psi(0)\rangle + \hat{P}_\downarrow e^{-iH(t-t_1)}\hat{P}_\downarrow e^{-iHt_1}|\psi(0)\rangle \quad (14)$$

$$\equiv |[\uparrow, \uparrow]\rangle + |[\uparrow, \downarrow]\rangle + |[\downarrow, \uparrow]\rangle + |[\downarrow, \downarrow]\rangle. \quad (15)$$

The last line just defines (term by term) a shorthand notation for the previous line. Each term represents a particular choice of projection at each time, and in that sense corresponds to a particular “path”. In the path integral formulation of quantum mechanics the time between projections is taken arbitrarily small, and the time evolution is viewed as a sum over microscopic paths. For present purposes, the time intervals can remain finite, representing a “coarse graining” in time. Each term in the above expression is called a “path projected state”, and the sum is a sum over coarse grained paths.

One attempts to assign the probability $\langle [i, j] | [i, j] \rangle$ to the path $[i, j]$, but to make sense, the probabilities must obey certain sum rules. For example, one can define

$$|[\uparrow, \cdot]\rangle \equiv |[\uparrow, \uparrow]\rangle + |[\uparrow, \downarrow]\rangle, \quad (16)$$

where the “.” signifies that *no* projection is made at t_1 . One would want the probability for the path $[\uparrow, \cdot]$ to be the sum of the probabilities of the two paths of which it is composed:

$$\langle [\uparrow, \cdot] | [\uparrow, \cdot] \rangle = \langle [\uparrow, \uparrow] | [\uparrow, \uparrow] \rangle + \langle [\uparrow, \downarrow] | [\uparrow, \downarrow] \rangle \quad (17)$$

However, one can “square” Eq (16) to give the general result:

$$\langle [\uparrow, \cdot] | [\uparrow, \cdot] \rangle = \langle [\uparrow, \uparrow] | [\uparrow, \uparrow] \rangle + \langle [\uparrow, \downarrow] | [\uparrow, \downarrow] \rangle + \langle [\uparrow, \uparrow] | [\uparrow, \downarrow] \rangle + \langle [\uparrow, \downarrow] | [\uparrow, \uparrow] \rangle \quad (18)$$

Only if the last two terms (the cross-terms) in Eq (18) are small is the sum rule (Eq (17)) obeyed. When the relevant sum rules are obeyed the paths are said to give “consistent” or “decohering” histories. Advocates of this

Table 1a		Table 1b	
path	value	path	value
$\langle \{\uparrow\uparrow\} \{\uparrow\uparrow\} \rangle$	0.70	$\langle \{II\} \{II\} \rangle$	0.74
$\langle \{\uparrow\downarrow\} \{\uparrow\downarrow\} \rangle$	0.00	$\langle \{I\perp\} \{I\perp\} \rangle$	0.03
$\langle \{\uparrow\cdot\} \{\uparrow\cdot\} \rangle$	0.70	$\langle \{I\cdot\} \{I\cdot\} \rangle$	0.61
% violation	0%	% violation	25%

Table 1: Testing the probability sum rule (Eq (15)) for different paths. For 1a the sum rules are obeyed for any choice of t_1 and t . For 1b, $t_1 = .035$ and $t = 0.06$

point of view argue that the only objects in quantum mechanics which make physical sense are sets of consistent histories. For a discussion of how this simple example links up with the (much more general) original work on this subject ([19, 20, 21, 22, 23]) see [18]. Other work on the consistent histories approach includes [24, 25, 26, 27, 28].

6 Testing for consistent histories

Table 1a checks the probability sum rule (Eq (17)) for the toy model whose evolution is depicted in Fig 1. The projection times are $t_1 = .15, t = .2$, and the projection basis is $\{|\uparrow\rangle, |\downarrow\rangle\}$. The sum rule is obeyed to the accuracy shown. In fact, using the $\{|\uparrow\rangle, |\downarrow\rangle\}$ projection basis, the sum rule is obeyed no matter which projection times are chosen and how frequently the projections are made.

This result came as a surprise to me. After all the interesting dynamics described in Figs 1 and 2, the consistent histories approach offers a completely static perspective. The constant “ \uparrow ” and “ \downarrow ” paths are consistent right through the period when the correlations are being set up.

One of the very interesting features of the consistent histories point of

view is that typically there are many different sets of consistent histories. It turns out that for this particular example some sets of consistent histories reflect the “quantum measurement” more directly.

Consider for a moment a static (Hamiltonian = 0) spin, not coupled to any apparatus. It turns out that as long as the same projection basis is chosen at t and t_1 , one always gets consistent histories. This is true for any projection basis. One could choose $\{|\uparrow\rangle, |\downarrow\rangle\}$ or one could choose the projection basis $\{|\mathcal{I}\rangle, |\perp\rangle\}$, where $|\mathcal{I}\rangle$ is the initial state of the spin ($a|\uparrow\rangle_2 + b|\downarrow\rangle_2$), and $|\perp\rangle$ is the state orthogonal to it. A static spin would naturally result in unit probability for the $[\mathcal{I}, \mathcal{I}]$ path, and zero probability for all other paths. Table 1b shows the results for the fully interacting spin, using the $\{|\mathcal{I}\rangle, |\perp\rangle\}$ projection basis, but otherwise the same as Table 1a. Clearly the sum rules are not obeyed in this case.

When $\{|\uparrow\rangle, |\downarrow\rangle\}$ was used as a projection basis, there was no difference, from the consistent histories point of view, whether the interactions between spin and apparatus were present or not. Consistent histories resulted in either case. When the $\{|\mathcal{I}\rangle, |\perp\rangle\}$ projection basis was used, the effects of the interactions were evident: Only in the absence of interactions were those histories consistent.

Gell-Mann and Hartle [23, 26] have emphasized the important role that “records” or correlations among subsystems can have in producing consistent histories. In [18] I noted that since the Schmidt decomposition gives an exact account of whatever correlations are present, the Schmidt states (eigenstates of the reduced density matrix) often make a very good choice of projection basis.

Indeed, I have found the following types of histories are always consistent for this toy system: For the first projection time one chooses the eigenstates of ρ_2 (the Schmidt states) as the projection basis. At the second projection time one chooses the $\{|\uparrow\rangle, |\downarrow\rangle\}$ projection basis. These paths are consistent for any choices of the two projection times. These paths certainly reflect the measurement process, since (as shown in Figs 1 and 2) this process shows up quite explicitly in the behavior of the Schmidt states. One can expand on this set of paths by including additional projections on the $\{|\uparrow\rangle, |\downarrow\rangle\}$ basis. However, one will not get consistent histories if one makes additional projections on the Schmidt basis (until after it coincides with the $\{|\uparrow\rangle, |\downarrow\rangle\}$ basis). Thus the actual picture presented by any of these sets of paths is quite different from the Schmidt paths depicted in Fig 1.

7 Time evolution and the density matrix

This section, and the one which follows, are devoted to describing how the Hamiltonian which governs the toy system is related to the results presented above.

To explore the effect of H_I , note that the initial state (Eq 8) can be written:

$$|\psi_i\rangle = a |\uparrow\rangle \otimes |X\rangle_1 + b |\downarrow\rangle \otimes |X\rangle_1. \quad (19)$$

Under time evolution according to H_I , this state maintains a similar form:

$$|\psi(t)\rangle = a |\uparrow\rangle \otimes |X_\uparrow(t)\rangle_1 + b |\downarrow\rangle \otimes |X_\downarrow(t)\rangle_1. \quad (20)$$

Where $|X_\uparrow(t)\rangle_1$ and $|X_\downarrow(t)\rangle_1$ are the initial apparatus state $|X\rangle$ evolved forward in time according to H_1^\uparrow and H_1^\downarrow respectively. Because H_1^\uparrow and H_1^\downarrow are different randomly chosen operators, on average the states $|X_\uparrow(t)\rangle_1$ and $|X_\downarrow(t)\rangle_1$ have no more overlap than two randomly chosen vectors in the apparatus subspace. For sufficiently large apparatus subspaces, the overlap will be extremely small.

From this point of view the initial conditions, where $\langle X_\uparrow(0)|X_\downarrow(0)\rangle = 1$, are very special. As time evolves the value of $\langle X_\uparrow(0)|X_\downarrow(0)\rangle$ decreases to its more natural small value. If $\langle X_\uparrow(0)|X_\downarrow(0)\rangle$ were to become close to unity later in time, this would correspond to the apparatus “forgetting” its records, analogous to the screen re-emitting an electron in a diffraction pattern state. In the toy model, this happens very rarely (for large apparatus) because two vectors evolving randomly in a large space rarely overlap. (This effect has been discussed at length in this context by Zurek [3].)

Much of the earlier discussion has focused on the eigenstates of the reduced density matrix for the spin (ρ_2), or Schmidt states. These states, along with the eigenvalues, provide the most concise description of the state of the spin, and they describe the correlations with the apparatus as well. The Schmidt states start out being very different from the the $\{|\uparrow\rangle, |\downarrow\rangle\}$ basis, but approach very close as the measurement is completed. The Schmidt states then stabilize close to the $\{|\uparrow\rangle, |\downarrow\rangle\}$ states and do not change much after the measurement.

The degree to which the Schmidt states are $\{|\uparrow\rangle, |\downarrow\rangle\}$ can be studied by examining the off diagonal matrix element of ρ_2 in the $\{|\uparrow\rangle, |\downarrow\rangle\}$ basis:

$$\langle \uparrow | \rho_2(t) | \downarrow \rangle = ab^* \langle X_\downarrow(t) | X_\uparrow(t) \rangle. \quad (21)$$

Equation 21 shows that to the extent that the overlap of $X_1(t)_1$ with $|X_1(t)_1$ is small, $\{|\uparrow\rangle, |\downarrow\rangle\}$ are the eigenstates of ρ_2 . As discussed in Appendix A, the typical overlap goes down as the size of the apparatus is increased, so even in this simple example one can see that large size is an advantage when building an apparatus.

7.1 A Catch

The case where a and b are nearly equal deserves special attention. In this case the eigenvalues of ρ_2 become nearly degenerate at late times, and the form of the eigenstates of ρ_2 becomes a delicate matter.

Consider first the case of strict equality:

$$a = b = 1/2 \tag{22}$$

In this limit $\langle \uparrow | \rho_2(t) | \uparrow \rangle = \langle \downarrow | \rho_2(t) | \downarrow \rangle = 1/2$, and the form of the eigenstates is completely determined by $\langle \uparrow | \rho_2(t) | \downarrow \rangle$. In this special case the eigenstates are either

$$\frac{(|\uparrow\rangle \pm e^{i\theta} |\downarrow\rangle)}{\sqrt{2}}, \tag{23}$$

if $\langle \uparrow | \rho_2(t) | \downarrow \rangle$ is non-zero (no matter how small!), or undetermined if $\langle \uparrow | \rho_2(t) | \downarrow \rangle$ is *exactly* zero. (See Appendix A for the definition of the phase θ and further details.)

A physicist need never worry about the “measure zero” case where Eq 22 is exactly obeyed, but there is a more general point to be made: As a and b get close to one another, even very small values of $\langle \uparrow | \rho_2(t) | \downarrow \rangle$ can be “too large” and cause the eigenstates of ρ_2 to deviate greatly from the desired $|\uparrow\rangle$ and $|\downarrow\rangle$ states.

In the toy system, the mean magnitude of $\langle \uparrow | \rho_2(t) | \downarrow \rangle$ is never zero, although it can be made arbitrarily small by increasing the size of the apparatus. Thus for every apparatus size there exists a limit to how close a and b can get without causing the Schmidt states to exhibit large deviations from the desired behavior. On the other hand, given any arbitrarily close values of a and b , there exists a sufficiently large choice of n_1 so that the desired behavior is achieved. In Appendix A I show that the minimum value of $|a - b|$ scales as $1/\sqrt{n_1}$. (Note that the “ n_1 ” of a real macroscopic apparatus is huge!)

I also argue in Appendix A that if one accepts the departure of $\langle \uparrow | \rho_2(t) | \downarrow \rangle$ from zero as an indication of the precision of the apparatus, then there is nothing particularly wrong with the apparatus in the $a \rightarrow b$ limit. The apparatus is just unable to precisely resolve the value of $a - b$. One could even argue that the sensitivity of the Schmidt basis to the precise value of $\langle \uparrow | \rho_2(t) | \downarrow \rangle$ in this limit makes the Schmidt basis misleading when $|a - b|$ falls below the “experimental resolution”. (This amounts to a major concession to W. Zurek, with whom I have been having ongoing informal debates about the value of the Schmidt decomposition!)

7.2 Some Red Herrings

I came up against the special behavior discussed in Section 7.1 early in the course of this work. Although I appreciated the overall delicacy of the degenerate eigenvalue case, my efforts to preserve the desired behavior in that limit were not always to the point. In this subsection I critique some remarks on this subject in previous papers of mine.

The eigenstates of H_I (from Eq 7) have the form of either:

$$|\lambda_I\rangle = |\uparrow\rangle \otimes |\lambda_1\rangle \quad (24)$$

or

$$|\lambda_I\rangle = |\downarrow\rangle \otimes |\lambda_1\rangle \quad (25)$$

where the $|\lambda_1\rangle$ and $|\lambda_1\rangle$ are the eigenstates of H_1^\uparrow and H_1^\downarrow respectively. The addition of sub-dominant “self-Hamiltonians” for the two subsystems does not have a large overall effect. However, frequently a handful of energy eigenstates deviate greatly from Eqs 24 and 25. (The reason is that among the random set of energy eigenvalues there are always a few which are quite close together. Under such circumstances small perturbations can greatly affect the form of the eigenstates, as was already discussed regarding ρ_2 .)

Some of my previous efforts to produce a “good measurement” in the $a \rightarrow b$ limit focused on avoiding the bad energy eigenstates, which are not close to Eqs 24 and 25. In [18] (section 6.1) I further reduced the coefficients of the self-Hamiltonians, and in [12] I specially chose the initial conditions to avoid the bad energy eigenstates. In fact none of these efforts were useful, because they did not reduce the overlap of $|X_1(t)\rangle_1$ with $|X_1(t)\rangle_1$. This overlap is present even when the energy eigenstates are exactly given by

Eqs 24 and 25, and the form of the eigenstates was not the problem which needed addressing. The overlap is most easily reduced in the toy system by increasing the the size (n_1) of the apparatus.

8 Consistent histories and the Hamiltonian

The states $|\uparrow\rangle$ and $|\downarrow\rangle$ for the spin are absolutely stable under the action of H_I . Once one projects with \hat{P}_\uparrow the projected state will remain of the form $|\uparrow\rangle \otimes |\text{something}\rangle_1$ from then on. Projecting with \hat{P}_\uparrow and \hat{P}_\downarrow at different times is certain to give zero. If $\{|\uparrow\rangle, |\downarrow\rangle\}$ is the projection basis, then the only path projected states with non-zero amplitude have all the projections either uniformly up or uniformly down (regardless of the values and frequency of the projection times). The only cross-term in Eq 18 which could potentially cause sum rule violation is the dot product between the uniformly up and uniformly down path projected states. This cross-term is also zero because $\langle \uparrow | \downarrow \rangle = 0$. Thus using the $\{|\uparrow\rangle, |\downarrow\rangle\}$ projection basis is sure to give consistent histories for this model, no matter what the initial state. Although these histories do not explicitly exhibit dynamics associated with the evolving correlations, their consistency is closely linked with these dynamics via the special stability of the $\{|\uparrow\rangle, |\downarrow\rangle\}$ basis. In Zurek's [3] language, the $\{|\uparrow\rangle, |\downarrow\rangle\}$ basis is a "pointer basis", which does not loose quantum coherence via the interactions.

The $\{|\uparrow\rangle, |\downarrow\rangle\}$ basis is special because of the form of H_I (Eq 7). The basis $\{|\mathcal{I}\rangle, |\perp\rangle\}$ is nothing special from the point of view of the Hamiltonian, and it is not surprising that consistent histories were not found using that projection basis.

The other sets of consistent histories discussed in Section 9 involved projecting first on the Schmidt states and then on the $\{|\uparrow\rangle, |\downarrow\rangle\}$ basis. After the first projection, the two resulting path projected states are just the two terms ($\sqrt{p_1}|1\rangle_2^S \otimes |1\rangle_1^S$ and $\sqrt{p_2}|2\rangle_2^S \otimes |2\rangle_1^S$) of the Schmidt decomposition of the total wavefunction at t_1 . The subsequent evolution of each path projected state may be treated as in Eq 20:

$$\begin{aligned}
 |[1](t) \rangle &= e^{-i(t-t_1)H_I} \left(\sqrt{p_1}|1\rangle_2^S \otimes |1\rangle_1^S \right) = |\uparrow\rangle \left(\sqrt{p_1} \langle \uparrow | 1 \rangle_2^S \right) \otimes |1_1(t)\rangle_1 \\
 &\quad + |\downarrow\rangle \left(\sqrt{p_1} \langle \downarrow | 1 \rangle_2^S \right) \otimes |1_1(t)\rangle_1 \quad (26)
 \end{aligned}$$

where $|1_{\uparrow}(t)\rangle_1$ and $|1_{\downarrow}(t)\rangle_1$ are $|1\rangle_1^S$ evolved under H_1^{\uparrow} and H_1^{\downarrow} respectively. Likewise:

$$\begin{aligned} |2\rangle(t) = e^{-i(t-t_1)H_I} \left(\sqrt{p_2}|2\rangle_2^S \otimes |2\rangle_1^S \right) &= |\uparrow\rangle \left(\sqrt{p_2} \langle \uparrow | 2 \rangle_2^S \right) \otimes |2_{\uparrow}(t)\rangle_1 \\ &+ |\downarrow\rangle \left(\sqrt{p_2} \langle \downarrow | 2 \rangle_2^S \right) \otimes |2_{\downarrow}(t)\rangle_1 \end{aligned} \quad (27)$$

Given the form of Eqs 26 and 27 it is easy to see the effect of later projecting on the $\{|\uparrow\rangle, |\downarrow\rangle\}$ basis. The resulting four path projected states are just the two terms from Eq 26 and the two terms from 27. The relevant cross-terms, which must be zero to give consistent histories are:

$$\langle \uparrow, 1 | \uparrow, 2 \rangle \propto \langle 1_{\uparrow}(t) | 2_{\uparrow}(t) \rangle \quad (28)$$

and

$$\langle \downarrow, 1 | \downarrow, 2 \rangle \propto \langle 1_{\downarrow}(t) | 2_{\downarrow}(t) \rangle \quad (29)$$

The quantity in Eq 28 is exactly zero because $|1_{\uparrow}(t)\rangle$ and $|2_{\uparrow}(t)\rangle$ started orthogonal, and were unitarily evolved by the same Hamiltonian, so they must remain orthogonal. Likewise for Eq 29.

Unlike the first set of consistent histories discussed, these histories are consistent because of orthogonality of the path projected states in the *apparatus* subspace. One can say that records of the spin at t_1 are present in the apparatus. The Schmidt decomposition (at t_1) was used to resolve these records. (If any other projection basis had been used at t_1 , the counterparts of $|1_{\uparrow}(t)\rangle$ and $|2_{\uparrow}(t)\rangle$ would *not* have started out orthogonal, and the cross-terms would not have come out zero.) The choice of second projection was also crucial. By choosing the stable $\{|\uparrow\rangle, |\downarrow\rangle\}$ basis, one avoided losing track of the records between t_1 and t_2 , when the second projections were made.

9 Comparing consistent histories with instantaneous probabilities

The consistent histories approach is all about assigning probabilities to histories. In contrast, the wavefunction at a *particular* time can be used to assign a probability to any state (possibly a state specified only for a subsystem). One just projects onto the state in question and squares to get the probability. This procedure can be repeated at different times (always

evolving the whole unprojected wavefunction). The Schmidt paths just give a way of following the probabilities assigned to a particular set of states. Often these Schmidt states are very interesting because they exactly reflect the correlations which are present.

The consistent histories and the instantaneous probabilities are in general very different from one another. However, the the two points of view can be quite similar in the particular case where good measurements are made within the closed system being treated. In that case projecting on a particular apparatus state should be completely equivalent to projecting (at an *earlier* time) on the corresponding state of the system being measured, as long as the projection is made at a time *after* the measurement has been completed (see for example refs [26, 24]). Since the Schmidt decomposition can be applied to expose the correlations among all the relevant apparatuses and systems, one might expect that the paths traced out by the Schmidt states *after* a measurement should bear a lot of resemblance to one set of consistent histories. However, based on the work in this paper, it does not seem that the consistent histories and the Schmidt paths bear much resemblance *during* the measurement process, when the correlations are actually being set up.

Much of this paper follows in the tradition of Zeh and Zurek, by analyzing the measurement process from the instantaneous probabilities point of view. It has rightly been pointed out [24, 23, 27, 29] that the information provided by a wavefunction at a single moment in time is of limited use in investigating many important issues in quantum mechanics. None the less, by following the *time development* of the instantaneous probabilities Zeh and Zurek have been able to provide some useful insights into the nature of the quantum measurement. (The whole notion of Zurek's "pointer basis"[3] or Zeh's "stability of the Schmidt states"[1] is connected with time evolution, as is the issue of "permanence" of the record, which both these authors address. Their analysis, which involves the time development of instantaneous probabilities, is very different from just looking at a wavefunction at a single moment in time.)

Like Zeh and Zurek, I have found the time development of the reduced density matrix to offer a convenient perspective on the measurement process. One can answer questions such as "how long does the measurement take?"[6], and "what is the state of the system half-way through the measurement?"(Fig 2). In turn these insights can help one deduce the features which make a good measurement apparatus.

In this particular application I have not found the consistent histories approach particularly illuminating. No single set of consistent histories appeared to be following the correlations in any continuous way, and no set of consistent histories indicated the duration of the measurement process. I have no doubt that by considering a large number of *different* sets of consistent histories one could generate this information, but not in a particularly direct way. In short, the time development of the reduced density matrix seems to allow one to focus more directly on the measurement process, as compared with the consistent histories point of view.

It is not at all clear that the different focus offered by the consistent histories is “bad”. After all, in many realistic situations one does not *want* to focus on the details of the measurement process. However, I have felt some informal (unpublished) pressure from a few consistent histories enthusiasts to completely abandon the reduced density matrix point of view. Anyone who wishes to take such a position ought to explain how the consistent histories give a superior perspective on the measurement process discussed here.

10 The arrow of time

As has been noted, for example by Zurek [3] and Zeh [30, 16, 31], there is an arrow of time built into the dynamics discussed here. This is dramatized in Fig 3, which is identical to Fig 1, but with the time axis extended to the interval $[-2, 2]$. One can see that the pure “initial” ($t = 0$) state (which has zero entropy for the spin), is a very special state and the “collapse of the wavefunction” proceeds in the direction of increasing spin entropy. The $t < 0$ part of Fig 3 illustrates an “un-collapsing” wavefunction, where the correlations present between spin and apparatus at early times are lost, and the pure state emerges at $t = 0$. Then, for positive values of t correlations are established again. The stability of these correlations (and thus the goodness of the measurement) depend on another such “entropy dip” not occurring for $t > 0$. In the language of Section 7, one is depending on the random evolution of $|X_1(t)\rangle_1$ and $|X_2(t)\rangle_1$ not to cause these two states to overlap appreciably at later times. (This issue has been discussed at length in [3].) Even the simple system discussed here is complex enough for such large entropy dips to occur very rarely. Still, with such a small apparatus, noticeable fluctuations are present. (Note that the portion of Fig. 3 which is shown in Fig 1 is

uncharacteristically well behaved. See Appendix C for further discussion.)

Aside from questions of stability, how fundamentally is the arrow of time linked to quantum measurement? The initial state, $|\psi_i\rangle$ has zero entropy for the spin, so it is not surprising that just about anything will cause the entropy to increase. What about starting with a more general initial state? Schmidt tells us that (in a suitable basis) the most general state can be written

$$|\tilde{\psi}_i\rangle = \sqrt{p_1}|1\rangle_2 \otimes |1\rangle_1 + \sqrt{p_2}|2\rangle_2 \otimes |2\rangle_1. \quad (30)$$

I show in Appendix B that if one requires evolution which generalizes Eq (9) to give

$$\begin{aligned} |\tilde{\psi}_i\rangle &\rightarrow |\tilde{\psi}_f\rangle \\ &= \sqrt{p_1}(\langle\uparrow|1\rangle_2|\uparrow\rangle \otimes |A\rangle_1 + \langle\downarrow|1\rangle_2|\downarrow\rangle \otimes |B\rangle_1) \\ &\quad + \sqrt{p_2}(\langle\uparrow|2\rangle_2|\uparrow\rangle \otimes |C\rangle_1 + \langle\downarrow|2\rangle_2|\downarrow\rangle \otimes |D\rangle_1) \end{aligned} \quad (31)$$

then one must have increasing (or constant) entropy of the spin ($-\text{tr}[\rho_2 \ln(\rho_2)]$) as $|\tilde{\psi}_i\rangle \rightarrow |\tilde{\psi}_f\rangle$. Thus “good measurement” appears to be closely linked with increasing entropy, even for high entropy initial states. (Note that I have chosen all four apparatus states, $|A\rangle_1$, $|B\rangle_1$, $|C\rangle_1$, and $|D\rangle_1$ to be mutually orthogonal. This means that in $|\tilde{\psi}_f\rangle$ the apparatus has a record of whether the spin is up or down, *and* which term of Eq (30) has been “measured”.)

11 Conclusions

The ideas put forward by Zeh [1], Zurek [3], Joos and Zeh [32], and Unruh and Zurek [7], have sufficiently de-mystified the notion of wavefunction collapse that one can actually unitarily follow the evolution of a system right through the collapse process. I have investigated a simple system which exhibits “wavefunction collapse”. I find Zeh’s idea of watching the evolution of the eigenstates of the reduced density matrix (Schmidt paths) particularly appealing. This approach allows one to follow exactly the evolution of the correlations among subsystems. It also allows one to visualize the collapse process quite explicitly, as illustrated in Fig 2. However, when eigenvalues of the reduced density matrix are nearly degenerate, the eigenstates become very sensitive to “noise”, and can give a misleadingly unstable picture of what is going on.

I also applied the “consistent histories” analysis (of Griffiths [19], Omnes [20, 21, 22] and Gell-Mann and Hartle [23]) to the same system. This approach allows one to consider many different sets of histories for the system. In the example studied here, many different sets passed the consistency test. It is intriguing that one set of consistent histories for the spin did not reflect the interesting evolution of the correlations between the spin and the apparatus. Instead, it was more a reflection of the stability properties of the spin. That set of histories would look the same for a static spin, decoupled from the apparatus. Other consistent histories exhibited more direct links to the “quantum measurement” process underway. However, there was very little resemblance between any given set of consistent histories and the Schmidt paths for the system. I argued that the reduced density matrix offered a more convenient point of view from which to analyze the measurement process.

I have employed a perspective on wavefunction collapse which explicitly does *not* make a choice among the possible outcomes at the end of the measurement process. This results in Everett’s “many worlds”. An advantage of this perspective is that the question of what makes a good apparatus can be addressed quite directly. To this end, I have discussed in detail the Hamiltonian used to evolve the system, and the features necessary to accomplish the desired evolution. Even in this primitive example, the quality of the apparatus is very clearly linked with its size, and with the statistical “irreversibility” associated with the thermodynamic arrow of time.

12 Acknowledgements

I would like to thank W. Zurek, M. Joyce, J. Halliwell and A.C. Albrecht for some very helpful discussions. This work was supported in part by the DOE and the NASA (grant NAGW-2381) at Fermilab.

A Nearly degenerate density matrices

A.1 Mathematics

Consider the matrix:

$$\begin{pmatrix} 1/2 + \delta & \omega^* \\ \omega & 1/2 - \delta \end{pmatrix}. \quad (32)$$

Its (un-normalized) eigenstates are:

$$\left\{ \left(\begin{array}{c} \frac{\delta - \sqrt{\delta^2 + \omega^* \omega}}{\omega} \\ 1 \end{array} \right), \left(\begin{array}{c} \frac{\delta + \sqrt{\delta^2 + \omega^* \omega}}{\omega} \\ 1 \end{array} \right) \right\}. \quad (33)$$

If one takes the limit $\omega \rightarrow 0$ while keeping δ fixed the eigenstates become proportional to $(0, 1)$ and $(1, 0)$. This is what the toy model is trying to accomplish for ρ_2 at late times, by making the off-diagonal terms (here ω) small. However, if one takes $\delta \rightarrow 0$ while keeping ω fixed the eigenstates become proportional to $(\pm \frac{|\omega|}{\omega}, 1)$. (Since ω corresponds to $\langle \uparrow | \rho_2 | \downarrow \rangle$, θ in Eq 23 is just the phase of $ab^* \langle X_1(t) | X_1(t) \rangle$.)

If one wants to require the eigenstates to be close to $(0, 1)$ and $(1, 0)$, one can require:

$$\frac{\delta - \sqrt{\delta^2 + \omega^* \omega}}{\omega} < \epsilon \quad (34)$$

for some small epsilon. For small values of $|\omega|/|\delta|$ Eq 34 becomes

$$\delta > \frac{\omega}{2\epsilon}. \quad (35)$$

This paper involves the case where ω is the overlap of two random vectors in a space of size n_1 . The magnitude of such a quantity is the net distance traversed by an n_1 -step random walk with average step size proportional to $\sqrt{n_1}$, so $\omega \propto 1/\sqrt{n_1}$. Combining this with Eq 35, one can see that the minimum allowed value of δ goes as $1/\sqrt{n_1}$.

A.2 Physics

The goal of the interactions was to get the wave function into the form given by Eq 9:

$$|\psi_f\rangle = a |\uparrow\rangle_2 \otimes |Y\rangle_1 + b |\downarrow\rangle_2 \otimes |Z\rangle_1 \quad (36)$$

with

$$\langle Y|Z\rangle = 0. \quad (37)$$

When $a \rightarrow b$ the Schmidt decomposition tells us that if one insists on Eq 37 holding exactly (which is what Schmidt does), then the Schmidt expansion can look very different than Eq 36. This is because even small non-zero values of $\langle X_1(0)|X_1(0)\rangle$ ($\equiv \omega$ in Eq 32) can have a large impact on the eigenstates in this limit. However, how *badly* does the wavefunction deviate from Eq 36 when $|\langle X_1(0)|X_1(0)\rangle| \gg |a - b|$ (that is, when $1 \gg \omega \gg \delta$ in Eq 32)? One check is to look at the “overlap” between actual reduced density matrix for the spin (ρ_2 given by Eq 32, for example) and the ideal result

$$\rho_1 \equiv \begin{pmatrix} 1/2 + \delta & 0 \\ 0 & 1/2 - \delta \end{pmatrix}. \quad (38)$$

The quantity $\text{tr}\sqrt{\rho_2\rho_1}$ is a good measure of the overlap which can be understood by writing each ρ in terms of its eigenstates[†]. The value of $\text{tr}\sqrt{\rho_2\rho_1}$ is unity when $\rho_2 = \rho_1$, and is zero when no eigenstates (with non-zero eigenvalues) overlap. Taking ρ_2 from Eq 32 and ρ_1 from Eq 38, and expanding for small ω (keeping δ fixed) one gets

$$\text{tr}\sqrt{\rho_2\rho_1} = 1 + O(\omega^2). \quad (39)$$

At least according to this measure, ρ_2 and ρ_1 are very close when ω is small, even when their eigenstates are very different.

One can further explore the suitability of the system as a “measurement apparatus” in the $a \rightarrow b$ limit by considering the interaction of a third system with the apparatus. One feature of a good apparatus is a “pointer”, which clearly exhibits the outcome of the measurement, and which can subsequently be measured by other systems to determine the outcome of the original measurement. (Zurek [3] emphasizes this point by clearly partitioning out the pointer from the rest of the apparatus). As discussed earlier, this feature is absent from the toy model.

For the sake of discussion I will force the issue by assuming there is a third system which has detailed information about $|X_1(t)\rangle$. It can use this information to suitably measure the apparatus. If the apparatus is found

[†]The square root of the operator $\rho_2\rho_1$ is defined in the usual way. The operator is expressed in its eigenbasis and the square root of its eigenvalues are taken.

in $|X_T(t)\rangle$ the third system will conclude that the spin is up. The issue is being “forced” only in the sense that one is asking the third system to know something very complicated (namely $|X_T(t)\rangle$, a complete “microscopic” state with messy time evolution) in order to use the apparatus. In a good apparatus some simple feature (such as a blip on a screen) should indicate the outcome.

So how much of a mistake does the third system make by using this procedure? The errors come because the overlap of $|\psi_f\rangle$ with $|X_T(t)\rangle$ receives contributions not just from the first term in Eq 20, which is indeed correlated with $|\uparrow\rangle$, but also from the *second* term (correlated with $|\downarrow\rangle$) due to the non-zero value of $\langle X_I(t)|X_T(t)\rangle$. To the extent that $\langle X_I(t)|X_T(t)\rangle$ is small, the errors are small *even* in the $a \rightarrow b$ limit. The size of $\langle X_I(t)|X_T(t)\rangle$ simply represents the precision of the apparatus.

Repeated measurements by the third system of identically prepared spin-apparatus systems should yield inferences of the values of a and b . These inferences should be increasingly good as the number of repetitions increases. The one “problem” encountered as $a \rightarrow b$ is that the actual value of $a - b$ falls below the precision of the apparatus. In this case the third system could only conclude that $a \approx b$ within the experimental uncertainties. As long as the precision of the apparatus is acceptable, there is *no* problem with the apparatus in the $a \rightarrow b$ limit.

However, by choosing to look at the Schmidt decomposition, one is looking at something which can be very sensitive to $a - b$, as illustrated at the beginning of this appendix. In the case where the magnitude of $a - b$ falls below the acceptable resolution of the apparatus, one could argue that the Schmidt decomposition can be very misleading. For example, the spin-apparatus system could be in a state sufficiently close to Eq 9 for practical purposes, but the Schmidt decomposition could yield something that looks completely different.

This more wary attitude toward the Schmidt decomposition represents a step back from the enthusiasm I have expressed on other occasions (see [18] at the very end of section 2.2, for example).

B Generalized measurements and the arrow of time

The point of this Appendix is to show that the final state in Eq 31 has higher entropy (relative to the spin-apparatus partition) than the generalized initial state given by Eq 30.

Equation 30 is manifestly in Schmidt form, and Eq 31 can be put in Schmidt form by collecting even and odd terms together. For the initial state, the eigenvalues of the density matrix are p_1 and p_2 . For the final state, the eigenvalues are

$$p_{\uparrow} = p_1 |\langle \uparrow | 1 \rangle_2|^2 + p_2 |\langle \uparrow | 2 \rangle_2|^2 \quad (40)$$

$$p_{\downarrow} = 1 - p_{\uparrow}. \quad (41)$$

The fact the ${}_1\langle A|C \rangle_1 = {}_1\langle B|D \rangle_1 = 0$ is important for obtaining Eq 40.

Since the entropy is monotonically decreasing in $|p_1 - p_2|$, it will suffice to show that $|p_{\uparrow} - p_{\downarrow}| \leq |p_1 - p_2|$. Without loss of generality I take $p_{\uparrow} > p_{\downarrow}$ and $p_1 > p_2$.

$$p_{\uparrow} - p_{\downarrow} = 2p_{\uparrow} - 1 = 2 \left(p_1 |\langle \uparrow | 1 \rangle_2|^2 + p_2 |\langle \uparrow | 2 \rangle_2|^2 \right) - 1. \quad (42)$$

Now define: $\Delta \equiv p_1 - p_2$. Using this definition and $p_1 + p_2 = 1$ one can rewrite Eq 42 as:

$$p_{\uparrow} - p_{\downarrow} = 2 \left(\frac{1 + \Delta}{2} |\langle \uparrow | 1 \rangle_2|^2 + \frac{1 - \Delta}{2} |\langle \uparrow | 2 \rangle_2|^2 \right) - 1 \quad (43)$$

$$= \Delta \left(|\langle \uparrow | 1 \rangle_2|^2 - |\langle \uparrow | 2 \rangle_2|^2 \right) \quad (44)$$

$$= \Delta \left(2|\langle \uparrow | 1 \rangle_2|^2 - 1 \right) \quad (45)$$

where the normalization condition $\langle \uparrow | \uparrow \rangle = |\langle \uparrow | 1 \rangle_2|^2 + |\langle \uparrow | 2 \rangle_2|^2 = 1$ was used in the final step. Since $(2|\langle \uparrow | 1 \rangle_2|^2 - 1)$ is manifestly bounded above by unity, the desired result, $|p_{\uparrow} - p_{\downarrow}| \leq |p_1 - p_2|$, is obtained.

C Search technique

Figure 1 is a “blow up” of a small portion of Fig 3. The reader might have noticed that the portion shown in Fig 1 is much closer to the “desired

behavior” than any other portion of Fig 3. This is due to the fact that I did a fair amount of fiddling around, trying to choose parameters which would make a good quantum measurement. The time range I looked at while searching parameter space was the same range used in Fig 1. Given this search “technique”, it is not surprising that my search ended on an atypical case. I stopped when I had found what I wanted (within the window of Fig 1). One could say that Fig 1 is slightly misleading. On the other hand, one could just as well say that I understand the apparatus: I am able to prepare it in a suitable manner so that a good measurement is performed, and the record is kept for a specified period (in this case, .2 units of time). Just about any apparatus must be dealt with in this way.

References

- [1] H. D. Zeh. *Found. of Phys.*, 3:109, 1973.
- [2] W. Zurek. *Phys. Rev. D*, 24:1516, 1981.
- [3] W.H. Zurek. *Phys. Rev. D*, 26:1862, 1982.
- [4] W.H. Zurek. Pointer basis and inhibition of quantum tunneling by environment-induced superselection. In *Proc. Int. Symp. Foundations of Quantum Mechanics, Tokyo*, page 181, 1983.
- [5] A. O. Caldeira and A. J. Leggett. *Physica*, 121A:587, 1983.
- [6] W.H. Zurek. Reduction of the wave packet: How long does it take? In *Frontiers of nonequilibrium statistical physics*. Plenum, 1986.
- [7] W. Unruh and W. Zurek. *Phys. Rev. D*, 40:1071, 1989.
- [8] W.H. Zurek. *Physics Today*, 44:36, 1991.
- [9] B.L. Hu, J.P. Paz, and Y. Zhang. *Phys. Rev. D*, 45:2843, 1992.
- [10] H. D. Zeh. There are no quantum jumps, nor are there particles. Heidelberg preprint, submitted to *Physics Letters A*, 1992.
- [11] H. Everett. *Rev. Mod. Phys.*, 29:454, 1957.

- [12] A. Albrecht. Two perspectives on a decohering spin. In J. Halliwell, editor, *The Physical Origins of Time Asymmetry*. Cambridge University Press, 1992.
- [13] E. Schmidt. *Math. Annalen*, 63:433, 1907.
- [14] E. Schrödinger. *Proc. Cambridge Phil. Soc.*, 31:555, 1935.
- [15] O. Kübler and H. D. Zeh. *Ann. Phys.*, 76:405, 1973.
- [16] H. D. Zeh. Quantum measurements and entropy. In W. H. Zurek, editor, *Complexity, Entropy and the Physics of Information*. Addison Wesley, 1990.
- [17] A.O. Barvinsky and A.Yu. Kamenshchik. *Class. and Quantum Gravity*, 7:2285, 1990.
- [18] A. Albrecht. Identifying decohering paths in closed quantum systems. *Phys. Rev. D* in press (FERMILAB-Pub-91/101-A), 1992.
- [19] R. Griffiths. *J. Stat. Phys.*, 36:219, 1984.
- [20] R. Omnès. *J. Stat. Phys.*, 53:893, 1988.
- [21] R. Omnès. *J. Stat. Phys.*, 53:933, 1988.
- [22] R. Omnès. *J. Stat. Phys.*, 53:957, 1988.
- [23] M. Gell-Mann and J. B. Hartle. Quantum mechanics in the light of quantum cosmology. In W. H. Zurek, editor, *Complexity, Entropy and the Physics of Information*. Addison Wesley, 1990.
- [24] J.B. Hartle. The quantum mechanics of cosmology. Lectures presented at the Jerusalem winter school on Quantum Cosmology and Baby Universes, 1990.
- [25] R. Omnes. *Ann. Phys.*, 201:354, 1990.
- [26] M. Gell-Mann and J. Hartle. In *Proceedings of the 25th international conference on high energy physics*, Singapore, 1991. World Scientific.

- [27] H.F. Dowker and J.J. Halliwell. The quantum mechanics of history: The decoherence functional in quantum mechanics. Preprint: MIT-CTP-2071, 1992.
- [28] R. Omnes. *Rev. Mod. Phys.*, 64:339, 1992.
- [29] Classical equations for quantum systems. UC Santa Barbara preprint UCSBTH-91-15, 1992.
- [30] H.D. Zeh. On the irreversibility of time and observation in quantum theory. In B. d'Espagnat, editor, *The Enrico Fermi School of Physics II*. Academic Press, 1971.
- [31] H.D. Zeh. *The Physical Basis for the Direction of Time*. Springer, Heidelberg, 1989.
- [32] E. Joos and H.D. Zeh. *Zeit. Phys.*, B59:223, 1985.

Figure Captions

Figure 1: a: The solid curve is $|\langle \uparrow | 1 \rangle^S|^2$, and the dashed curve gives $\langle \uparrow | \rho_2 | \uparrow \rangle$.
b: The solid curve is the largest eigenvalue of ρ_2 , the dashed curve is the entropy of the spin.

Figure 2: “A collapsing wavefunction.” Each plot depicts an eigenstate of ρ_2 in terms of $p(\uparrow) \equiv |\langle \uparrow | i \rangle|^2$ and $p(\downarrow) \equiv |\langle \downarrow | i \rangle|^2$. The columns correspond to three different times. The two rows correspond to the two eigenstates.

Figure 3: The same plots as Fig 1 extended over a wider time range.

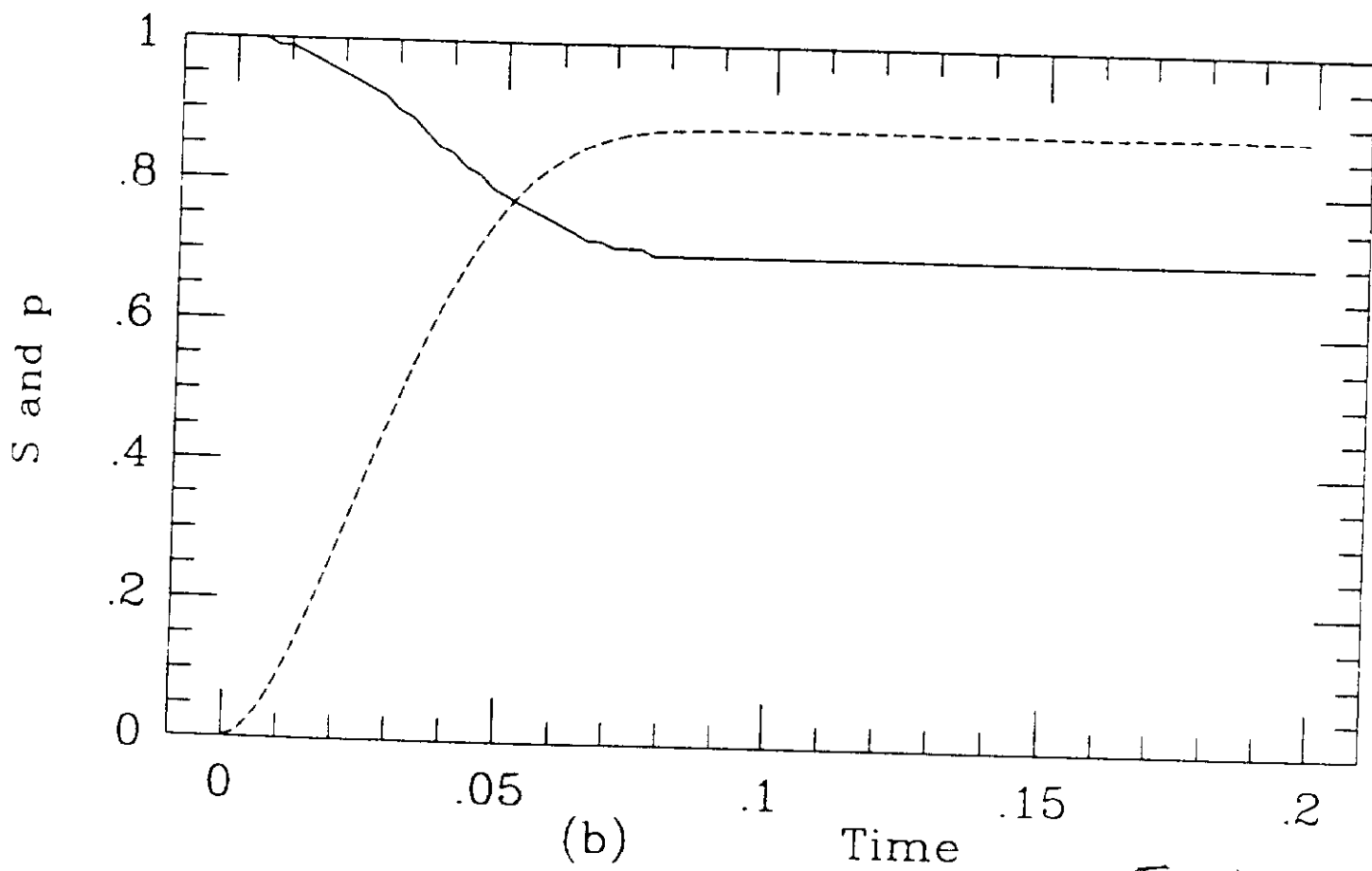
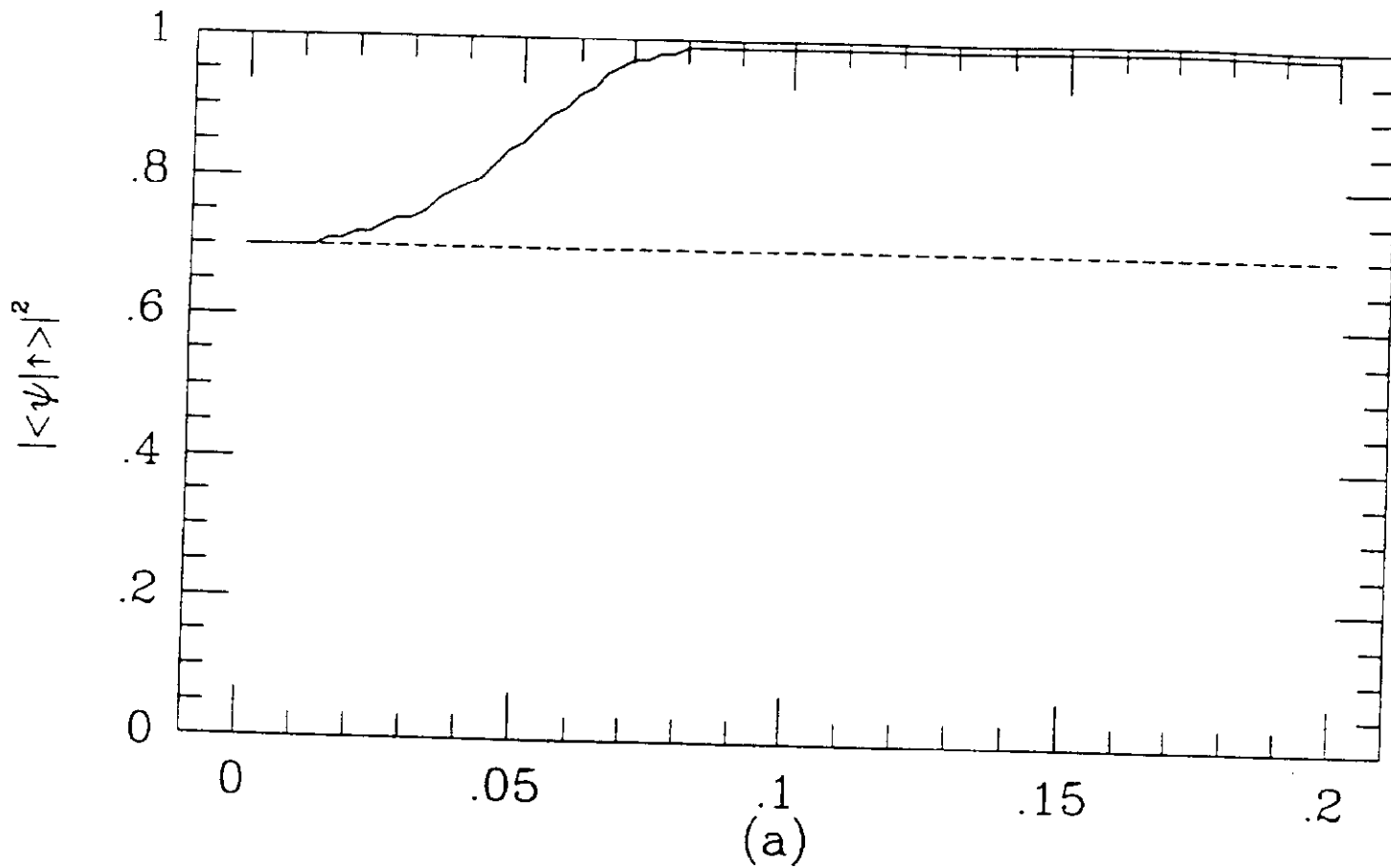
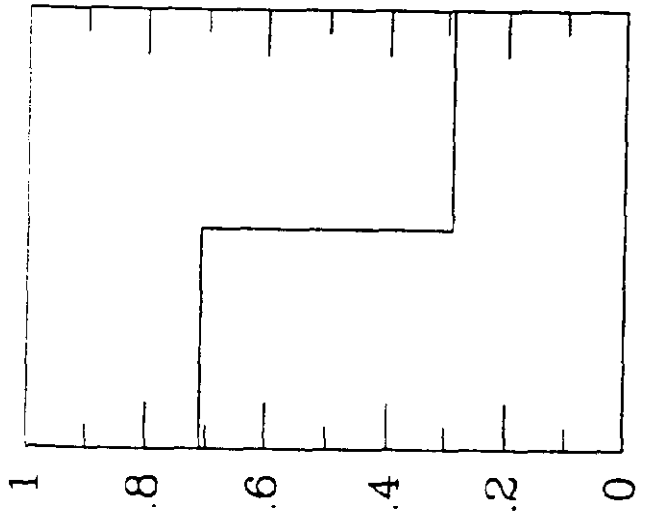
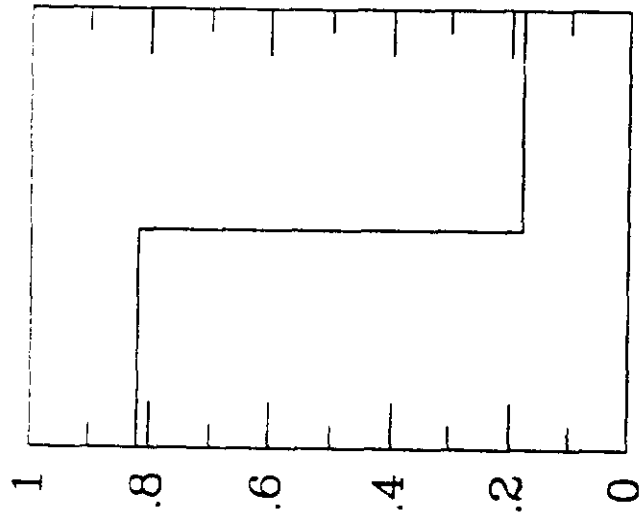


Fig 1



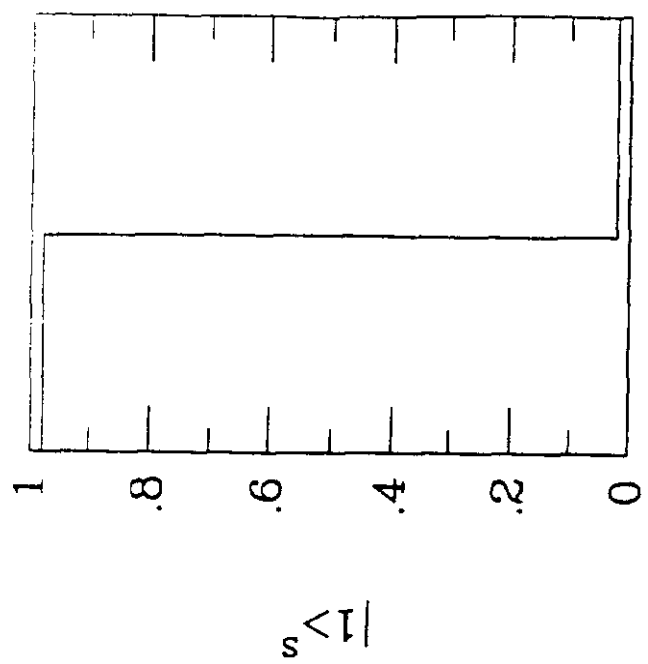
$P(\uparrow) P(\downarrow)$

$t = 0$



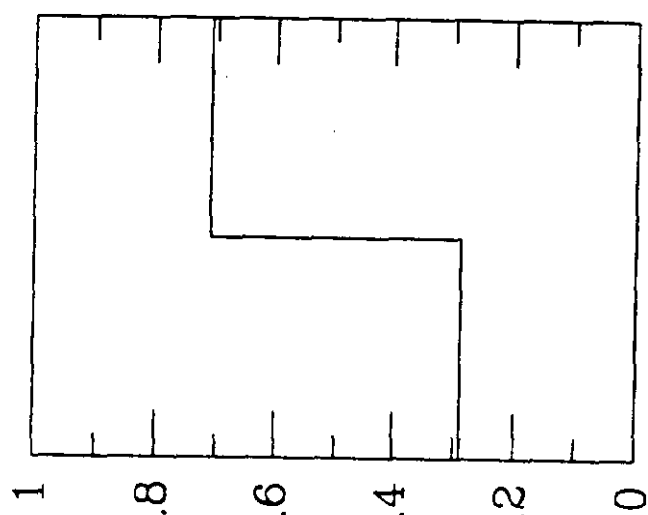
$P(\uparrow) P(\downarrow)$

$t = 0.03$

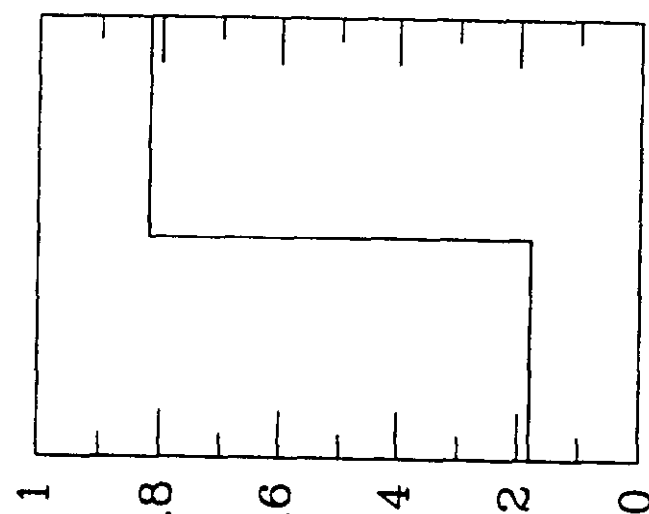


$P(\uparrow) P(\downarrow)$

$t = 0.15$

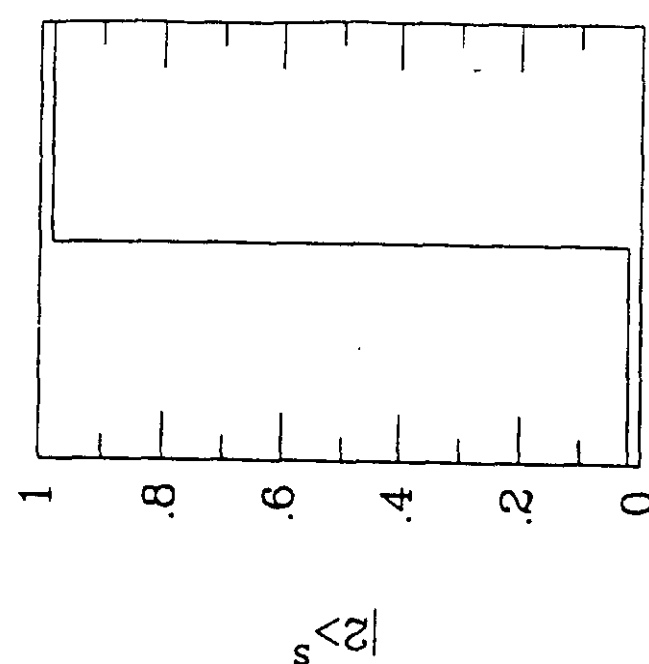


$\overline{|2\rangle_s}$



$P(\uparrow) P(\downarrow)$

$t = 0.03$



$\overline{|2\rangle_s}$

$P(\uparrow) P(\downarrow)$

$t = 0.15$

Fig 2

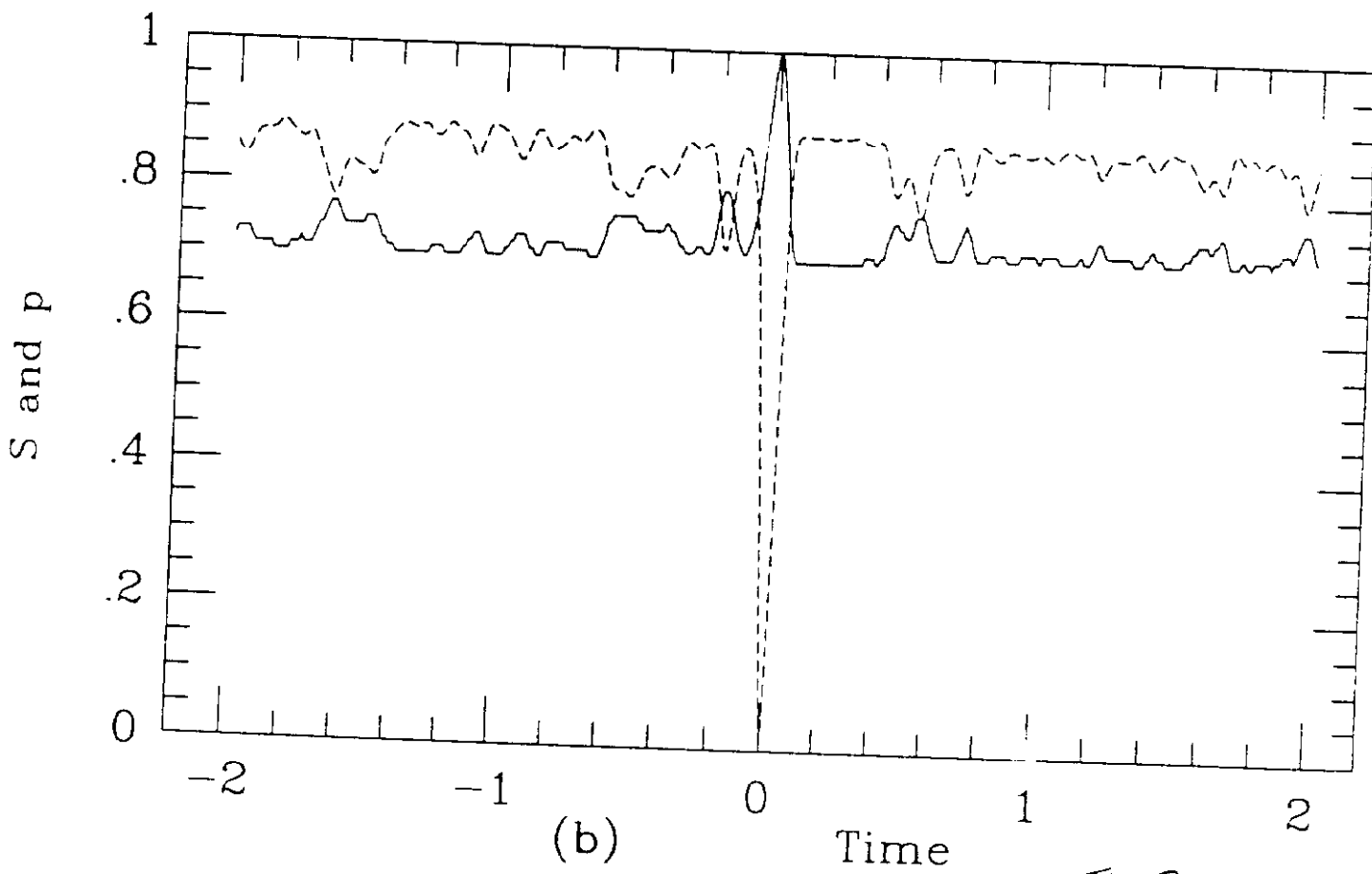
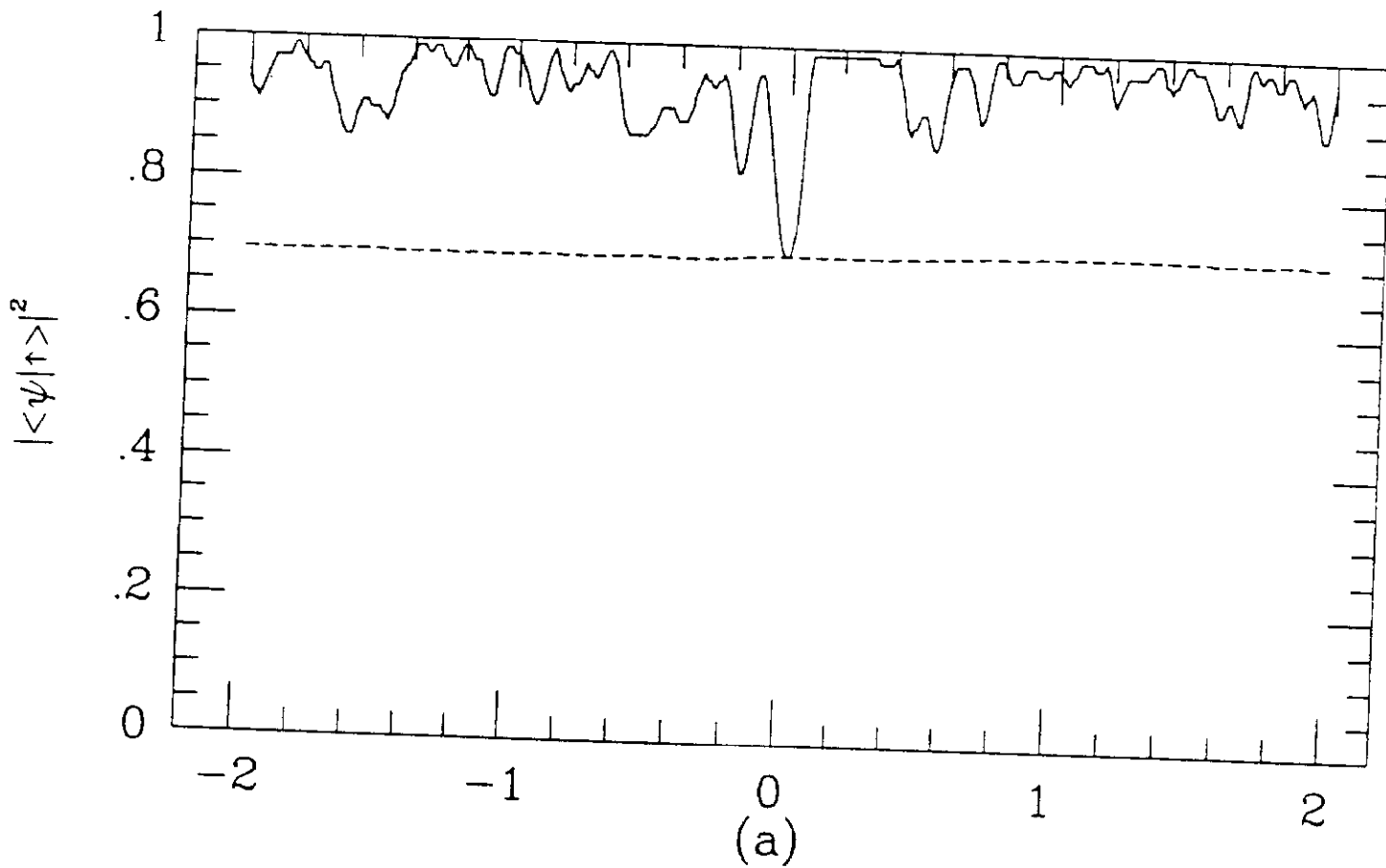


Fig 3